Conformation of Free Linear Polymer Chains in a Polymer Network

Xiaodu Liu,[†,‡] Barry J. Bauer,[§] and Robert M. Briber*[,†]

Department of Materials and Nuclear Engineering, University of Maryland, College Park, Maryland 20742-2115, and Polymers Division, National Institute of Standards and Technology, Gaithersburg, Maryland 20899

Received June 14, 1996; Revised Manuscript Received April 29, 1997[⊗]

ABSTRACT: Small angle neutron scattering has been used to measure the radius of gyration of deuterated linear polystyrene at dilute concentration contained in a polystyrene network with different crosslink densities. At each crosslink density, four samples with different linear chain concentrations (less than the overlap concentration) were made. The lower crosslink density samples (N_c >180) remained single phase, while higher crosslink density samples showed evidence of phase separation. Zimm plots were made for all samples which were single phase, and the second virial coefficient was obtained as a function of crosslink density. It was found that the second virial coefficient decreased with increasing crosslink density. Single chain form factors were obtained by extrapolating the scattering data to zero concentration of the linear chain for the single phase samples. A modified Debye equation was used to fit the zero concentration extrapolated scattering data over the entire experimental q range to obtain the radius of gyration, R_g, for the linear chain. It was found that R_g was a function of the crosslink density. When the crosslink density was low ($N_c > N_l$), R_g did not change appreciably and had a value nearly the same as in the melt. For higher cross-link density samples ($N_c < N_l$), R_g was found to decrease with increasing crosslink density and the scaling relation $R_g^{-1} \sim N_c^{-1}$ was observed. Chain segregation was observed for the highest crosslink density samples. The dependence of R_g on crosslink density can be qualitatively explained using a theory for the conformation of polymer chain in a random media. For the phase separated samples, a two correlation length theory was used to fit the scattering data.

Introduction

The conformation of an isolated linear polymer chain trapped in a network is an important problem in the field of polymer physics. In addition to shedding light on the interaction between the linear chain and the network matrix, this problem is related to problems in other fields such as diffusion of linear polymer chains (in a network), gel permeation chromatography, polymer chain transport through membranes and porous structures, and gel electrophoresis.[1−11] If the crosslink points in a polymer network can be equated to quenched random obstacles, the conformation of a polymer chain in a network can be related to the conformation of a linear chain in a quenched random medium. A quenched random medium is defined as a medium containing obstacles randomly distributed in space and fixed in position (i.e. quenched). A number of theories and computer simulations have been published in the literature describing polymer chain conformation in such media.[12−20] In general, it has been found that the radius of gyration, R_g, depends on the obstacle density. In the work by Muthukumar et al.[14,16−17] it was found that for Gaussian chains, when the density of obstacles is low, there is a transition when from a self-avoiding polymer chain (i.e. a chain exhibiting excluded volume effects) to an ideal Θ statistics. The existence of the quenched random obstacles reduces the strength of the excluded volume effects (equivalent to lowering the quality of the matrix solvent). When the density of obstacles is higher, a transition from a Gaussian chain to a localized collapsed chain occurs. Gersappe et al.[18] have shown by computer simulation that the chain statistics remain the same in the presence of the obstacles and the changes in R_g with increasing obstacle density operate only though the prefactor for R_g. In the Monte Carlo lattice simulation by Honeycutt and Thirumalai,[19] it was shown that polymer chains in a porous media collapse and the collapsed polymer chains (located in obstacle-free regions) were considerably more spherical (less anisotropic) than random coils. Although many of the details of the systems examined in the theoretical work mentioned above differ, it has generally been found that the R_g shrinks in the presence of random obstacles.

Although there are a number of theoretical studies and computer simulations in the literature, only a few experiments related to this problem have been performed. In the small angle scattering (SANS) work by Boué et al.,[21] it was found that the R_g of the free linear chains was equivalent to that found in the melt for linear chains which were the same as the length of network strands. In the work by Wu and Jong,[22] the R_g of the linear chains was measured by SANS using contrast variation and was observed to be smaller than in the corresponding uncrosslinked melt, although for most of the samples the linear chains appeared to be segregated. Recently, Horkay et al.[23] also observed a significant decrease in the R_g of trapped chains in a solvent swollen crosslinked polymer by SANS. In all of these previous experiments, only a few crosslink densities were studied. In the work reported here, SANS was used to measure the R_g of deuterated linear polystyrene (PSD) chains trapped in a protonated polystyrene (PSH) network as a function of crosslink density. A broad range of crosslink densities was studied, covering mesh sizes from much larger to much smaller than the length of the linear chain. The linear chain concentrations for all of the samples were less than ϕ^* (the overlap concentration) to eliminate inter-

* To whom correspondence should be addressed.
† University of Maryland.
‡ Current address: Department of Chemical Engineering, Lehigh University, Bethlehem, PA 18015.
§ National Institute of Standards and Technology.
⊗ Abstract published in *Advance ACS Abstracts,* July 15, 1997.

S0024-9297(96)00864-9 CCC: $14.00

chain interactions. The single chain form factor was obtained from the SANS data by extrapolation to zero linear chain conformation.

Theory

A. Measurement of Single Chain Form Factor by SANS for Dilute Mixtures. Among other things, SANS can be used to study both the morphology in a phase separated polymer mixture and the polymer chain conformation in a single phase system. The single chain scattering factor can be obtained from SANS data by using theories which have been developed over the years.[24−27]

Using the Flory−Rehner swelling theory,[28,29] the free energy of a swollen network containing free linear polymer chains can be written as

$$\frac{\Delta f}{kT} = \frac{3}{2v_c N_c}(\phi_s^{2/3}(1-\phi_l)^{1/3} - 1 + \phi_l) + \frac{(1-\phi_l)}{2v_c N_c}\ln\left[\frac{1-\phi_l}{\phi_s}\right] + \frac{\phi_l \ln \phi_l}{\phi_l N_l} + \frac{\chi}{v_0}\phi_l(1-\phi_l) \quad (1)$$

where ϕ_l is the volume fraction of the linear chain; ϕ_s is the volume fraction where the network is relaxed (i.e. reference state of the network which is usually taken as the volume fraction where the network was formed[25]); N_c is the average number of repeat units between crosslink points in the network; N_l is the average number of repeat units in the linear chain; v_l, v_c, and v_0 are the molar volumes of the network repeat unit, linear chain repeat unit, and reference volume for the lattice, respectively (usually v_0 is given as $(v_c v_l)^{1/2}$); and χ is the Flory−Huggins interaction parameter. The chemical potential of the linear chain in the network is given by $\Delta\mu_1 = \partial(\Delta F/kT)/\partial n_l$, where the ΔF is the total free energy of the system and n_l is the number of moles of the linear chain in the network. Swelling equilibrium is reached when the chemical potential of the linear chains in the network is equal to the chemical potential of pure linear chains. Accounting for concentration fluctuations in the already swollen network[30] and assuming $\phi_s = (1 - \phi_l)$, the zero angle scattering can be calculated as

$$\frac{k_n}{I(0)} = \frac{3}{2v_c N_c(1-\phi_l)} + \frac{1}{v_l N_l \phi_l} - 2\frac{\chi}{v_0} \quad (2)$$

where k_n is the contrast factor for neutron scattering.

For small ϕ_l, eq 2 can be written as a virial expansion

$$\frac{k_n \phi_l}{I(0)} = \frac{1}{v_l N_l} + 2A_2\phi_l \quad (3)$$

where the A_2 is the second virial coefficient and is given by

$$A_2 = \frac{3}{4v_c N_c} - \frac{\chi}{v_0} \quad (4)$$

This is consistent with the classical Zimm equation,[24,25,31,32] which describes the scattering from a dilute concentration polymer mixture:

$$\frac{k_n \phi_l}{I(q)} = \frac{1}{v_l \langle N_l\rangle_n \langle P_l(q)\rangle_w} + 2A_2\phi_l \quad (5)$$

where $I(q)$ is the measured scattering intensity, $\langle P_l(q)\rangle_w$ and $\langle N_l\rangle_n$ are the weight average single chain form factor and the number average degree of polymerization. In the limit of infinite dilution ($\phi_l \to 0$), the effect of A_2 is eliminated and eq 5 reduces to the single chain form factor:

$$\lim_{\phi_l \to 0}\left[\frac{I(q)}{k_n \phi_l}\right] = v_l \langle N_l\rangle_n \langle P_l(q)\rangle_w \quad (6)$$

For a polymer with a Zimm−Schulz molecular weight distribution,[25,33] $\langle P_l(q)\rangle_w$ can be written as[34]

$$\langle P(q)\rangle_w = \frac{2}{\langle x\rangle_n^2}\left[\langle x\rangle_n - 1 + \left[\frac{h}{h + \langle x\rangle_n}\right]^h\right] \quad (7)$$

where $\langle x\rangle_n = (R_g q)^2$ and R_g is the number average radius of gyration, $h = 1/(\langle N\rangle_w/\langle N\rangle_n - 1)$, and $\langle N\rangle_w$ is the weight average degree of polymerization. Equation 5 is used to extrapolate the experiment scattering data to the limit of $\phi_l \to 0$ (infinite dilution) for all values of q to obtain $\lim_{\phi_l \to 0}(I(q)/k_n\phi_l)$ (the single chain form factor). This allows the nonlinear fitting of eq 6 to the data using all values of $I(q)$ to obtain R_g rather than the traditional low-q Zimm approximation.

B. Radius of Gyration of Linear Chains in a Matrix of Quenched Random Obstacles. A calculation by Edwards and Muthukumar,[14,16,17] showed that when the attractive interactions arising from the obstacles dominate over the excluded volume contributions, the radius gyration of free linear chains in a quenched random medium is a function of the obstacle density:

$$R_g^2 = \frac{1}{6C\rho^2 b^4}(1 - e^{-C\rho^2 b^6 N_l}) \quad (8)$$

where ρ is the density of the obstacles, b is the statistical segment length, and $C = eu^2$ (e is a constant and u is a positive interaction constant between the polymer segment and the obstacles). If the obstacles correspond to the crosslink points of the polymer network and $2N_c >> 1$, then we expect $\rho \approx 1/2v_c N_c$. By substituting this relation into eq 8, the radius of gyration, R_g, can be rewritten as a function of N_c and for the limiting cases:

$$R_g^{-1} = \begin{cases} \left[\frac{b^2 N_1}{6}\right]^{-1/2} \sim \frac{1}{R_g(\Theta)} & \text{for the case where } \frac{(bN)^{1/2}}{N_c} \to 0 \ (N_c \text{ large or } N_1 \text{ small}) \\ \left[\frac{2(v_c N_c)^2}{3Cb^4}\right]^{-1/2} \sim \frac{1}{N_c} & \text{for the case where } \frac{(bN)^{1/2}}{N_c} \to \infty \ (N_c \text{ small or } N_1 \text{ large}) \end{cases} \quad (9)$$

where $R_g(\Theta)$ is the radius of gyration of the linear chain at Θ conditions. This predicts that as the obstacle density increases, the chain undergoes a crossover from the Gaussian state to a localized state where the inverse of the radius of gyration is proportional to the inverse of N_c.

C. SANS from Two Phase Polymer Mixtures. For an incompressible, randomly distributed two phase polymer system with sharp interfaces, the scattering intensity can be obtained as[35,36]

$$I(q) = \frac{8p\xi^3\phi_S(1-\phi_S)k_n}{(1+q^2\xi^2)^2} \quad (10)$$

where ϕ_S is the volume fraction of phase separated component and ξ is the Debye−Bueche correlation length, which is related to the size of the heterogeneities. According to eq 10, a plot of $I(q)^{-1/2}$ versus q^2 should give a straight line.

For two phase polymer systems with complex morphologies, a deviation from linearity in the low-q region is often observed in $I(q)^{-1/2}$ versus q^2 plots.[37−39] In order to account for this, the Debye−Bueche analysis has been modified and a two-correlation length model has been proposed.[37] The scattering intensity based on this two-correlation length model can be calculated as

$$I(q) = \frac{B_1}{(1+q^2\xi_1^2)^2} + B_2 \exp\left[-\frac{q^2\xi_2^2}{4}\right] \quad (11)$$

where $B_1 = 8\pi\xi_1^3 f\phi_s(1-\phi_s)k_n$, $B_2 = \pi^{3/2}\xi_2^3(1-f)\phi_s(1-\phi_s)k_n$, ξ_1 is the short-range correlation length, ξ_2 is the long-range correlation length, and the parameter f is the fractional contribution of the short-range correlation length to the total correlation function which can be calculated as $f = B_1/[B_1 + 8/\pi^{1/2}(\xi_1/\xi_2)^3 B_2]$. The f parameter provides the information of the distribution of second phase domains in the bulk materials. The case of $f = 1$ corresponds to where the second phase domains are distributed in space uniformly, and $0 < f < 1$ refers to where the second phase is heterogeneously distributed. The average size $\langle l_c \rangle$ and the average volume $\langle v \rangle$ of the second phase domains can also be calculated from the two-correlation lengths and the f parameter which is given as $\langle l_c \rangle = 2f\xi_1 + (1-f)\xi_2\pi^{1/2}$ and $\langle v \rangle = 8f\xi_1^3 + (1-f)\pi^{1/2}\xi_2^3$.

Experimental Section

A narrow molecular weight distribution, anionically polymerized, deuterated linear polystyrene (PSD) was obtained from Polymer Labs, Inc., with $M_w = 85\,000$ and $M_w/M_n = 1.02$.[40] The styrene monomer and divinylbenzene were purchased from Aldrich Chemical Co. The linear deuterated polystyrene was then dissolved in styrene monomer containing a small amount of divinylbenzene (DVB) as the crosslinking agent. Free radical polymerization using AIBN as the initiator was performed to form the polystyrene network around the linear chains. The polymerization was done using the following temperature history: 3 h at 50 °C, 3 h at 60 °C, 12 h at 70 °C, and another 3 h at 130 °C. By varying the amount of the divinylbenzene, nine different crosslink densities were synthesized (see Table 1). For each crosslink density, four different concentrations of linear chains were made. In all cases, the concentration of the linear chains was less then the overlap concentration ϕ^*. After polymerization, the samples were cut and polished into disks suitable for SANS (1 mm in thickness and 14 mm in diameter). The samples were sandwiched by two quartz windows and placed in brass sample cells. Before the neutron scattering, all of the samples were annealed at 120 °C for about 24 h.

The crosslink densities of the samples were calculated from the stoichiometry of the divinylbenzene, and the results were checked by swelling.[41] The toluene was used as the swelling solvent, and the Flory−Huggins interaction parameter for polystyrene/toluene at room temperature was taken as 0.40.[42] The final crosslink densities were calculated by averaging the results of stoichiometry and swelling measurements (Table 1).

The 30 m SANS instrument at the Cold Neutron Research Facility (CNRF) at the National Institute of Standards and Technology (NIST) was used for the scattering experiments. In this study, the incident neutron wavelength was 5 Å, and the wavelength resolution, $\Delta\lambda/\lambda \sim 0.15$, where λ is the wavelength of the neutron beam and $\Delta\lambda$ is the full width at half-maximum. The data were not desmeared for instrumental resolution. A two-dimensional detector was used to collect the scattering data. The samples were kept at 140 ± 0.2 °C (above the polystyrene glass transition temperature) for the SANS experiment. The observed scattering intensity was corrected for background scattering, sample transmission and thickness, empty cell scattering, cell by cell variation of the detector efficiency, and the incoherent scattering.[43] The intensity was then converted to an absolute scale using a secondary intensity standards calibrated at NIST.[58] The corrected two-dimensional data were then circularly averaged to obtain the dependence of scattering intensity on the wave vector ($q = (4\pi/\lambda)\sin(\theta/2)$, where θ is the scattering angle). Error bars were calculated on the basis of the standard statistical analysis of the fits to the data and represent 2 standard deviations. Error bars on calculated quantities were based on standard propagation of errors.[44]

Table 1. Radius of Gyration, Second Virial Coefficient, and the Chain Expansion Factor as a Function of N_c[a]

sample	N_c	R_g Å	$A_2 \times 10^5$, mol/cm^3	$\alpha = R_g/R_g(\Theta)$
1	∞	70.8 ± 0.4	0.55 ± 0.26	1.00
2	740	70.1 ± 0.4	−1.63 ± 0.41	0.99
3	640	66.8 ± 0.5	−1.44 ± 0.50	0.94
4	340	64.3 ± 0.7	−7.22 ± 0.90	0.91
5	260	62.0 ± 0.6	−8.58 ± 1.12	0.88
6	180	*b*	*b*	*b*
7	100	*b*	*b*	*b*
8	50	*b*	*b*	*b*

[a] $M_w = 79\,200$; $M_w/M_n = 1.02$. [b] The linear chains have segregated in these samples.

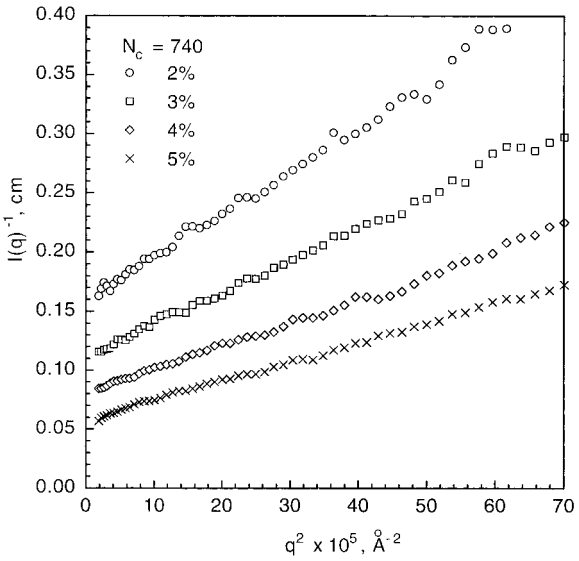

Figure 1. Ornstein−Zernike plot for the sample with $N_c = 740$.

Results and Discussion

A. Discussion of Compatibility. The scattering intensity in the low-q range for a single phase binary polymer blend should follow the Ornstein−Zernike equation,[45,46] and a plot of $1/I(q)$ versus q^2 should give a straight line. In this experiment, it was found that for samples with $N_c > 640$ the $1/I(q)$ versus q^2 plots do show linear behavior, but for samples with $N_c < 260$ a significant increase in the scattering intensity at the low-q region was observed. For samples with $N_c = 260$ and 340, only the lowest concentration samples show linear behavior. Nonlinear behavior implies that segregation of the linear chains had occurred. Figures 1 and 2 are $1/I(q)$ versus q^2 plots for samples with $N_c = 740$ and $N_c = 180$ showing the two types of behavior.

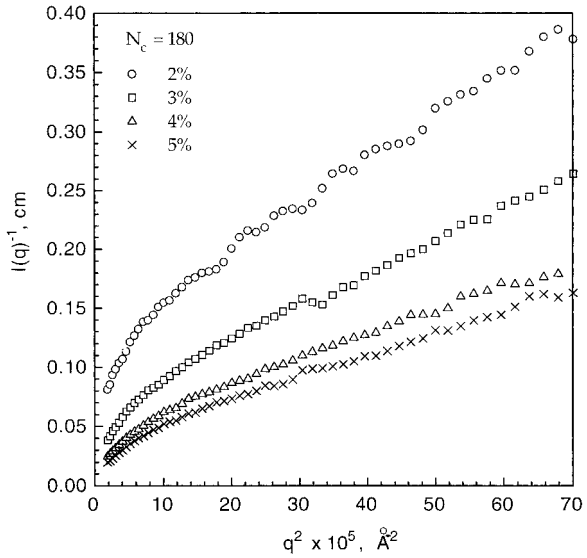

Figure 2. Ornstein−Zernike plot for the sample with N_c = 180.

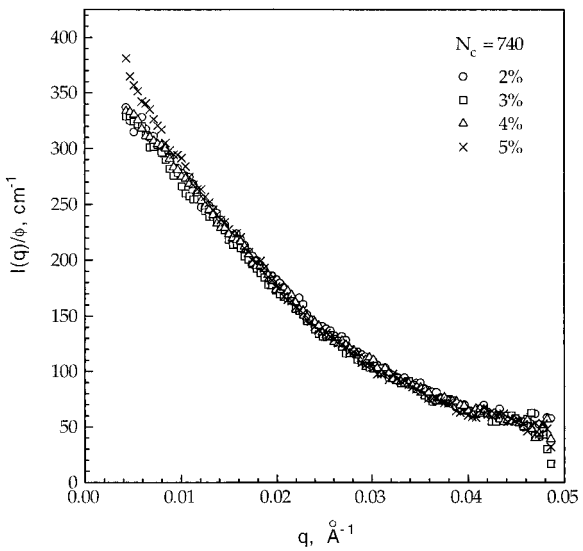

Figure 3. $I(q)/f_l$ versus q for the samples with N_c = 740.

Although classical rubber elasticity can be used to calculate the expected degree of swelling for a particular crosslink density network swollen by a given molecular weight linear chain, one cannot predict the observed phase separation point for the materials on the basis of this model. Classical theory defines a reference state of the network (ϕ_s in eq 1) which represents the volume fraction where the network is relaxed (i.e. not subject to swelling forces). Generally this is taken to be the volume fraction where the network is formed, which leads to the condition that the network chains should be relaxed at the end of the polymerization (even in the presence of the unattached linear chains). If the network is truly relaxed under the conditions of synthesis, then phase separation should not occur with increasing crosslink density or increasing length of the linear chain, as has been observed in this work and other studies involving networks containing linear chains or for networks polymerized in solution.[21,22] No theoretical or practical way of dealing with the problem of determining the reference state of the network has been determined. Consequently, on the basis of the traditional view of swelling theory, the samples in this work would not have been expected to phase separate even at high network densities if the network were in the relaxed state as polymerized. Clearly other factors beyond the traditional theory are required, such as where the conformation of the chain is altered due to the presence of the crosslinks (i.e. random obstacles).

It should also be pointed out that the phase separation observed in this experiment was not driven by the isotope effect, which leads to a small positive interaction parameter between deuterated and protonated polystyrene, χ_{H-D}.[45] The critical value of χ_s/v_0 for phase separation in the limiting case of infinite molecular weight of one component (i.e. a network) can be estimated from the equation for the spinodal based on the Flory−Huggins free energy of mixing by taking the limit as the molecular weight of one species becomes infinite and is given by $\chi_s/v_0 = {}^1/_2\phi_l N_l v_l$. The critical value for the highest concentration of linear chain studied in this work (ϕ_l = 5%) is $\chi_s/v_0 \cong 1.33 \times 10^{-4}$ mol/cm^3, which is significantly larger than the value reported for χ_{H-D} ($\chi_{H-D}/v_0 \approx 2 \times 10^{-6}$ mol/cm^3). This indicates that the isotope effect should not be a significant influence on the segregation of the linear chains in this work.

It should be noted that another possible explanation for the phase separation is that the crosslinking agent (DVB) is chemically different from the PS. This might give rise to an additional enthalpic interaction to the crosslink points. This should be a small effect, and on the basis of copolymer theory one would expect this interaction to scale as $\sim\phi_{DVB}^2$ or $1/N_c^2$, which, for the relatively low levels of crosslinking used in this study, should not play an important role.

B. Analysis of Single Phase Samples. The scattering curves for the samples with N_c = 740 are given in Figure 3. The scattering intensity was normalized by dividing by the linear chain concentration. The normalized scattering curves do not completely overlap with each other due to an effective second virial coefficient, A_2, which is not zero. In order to obtain the single chain form factor, the effect of A_2 needs to be eliminated by extrapolating to zero concentration. Equation 5 was used to do this extrapolation, and the zero concentration extrapolated scattering data were obtained over the full q range.

Once the zero concentration extrapolated data were obtained, eqs 6 and 7 were used to fit the data for the single phase samples over the entire q range by nonlinear regression to obtain a best fit R_g. The data for the uncrosslinked sample ($N_c = \infty$) were fit first, and the best fit linear chain molecular weight and unperturbed radius of gyration, N_l^∞ and R_g^∞, were obtained. The value of N_l^∞ was then held constant in fitting the data for the crosslinked samples to obtain R_g. The results are presented in Table 1. The zero concentration extrapolated scattering curve for the sample with N_c = 740 and the fit are shown in Figure 4.

In the limit of small q, eq 7 can be expanded which can be substituted into eq 5, which can be rewritten as

$$\frac{k_n\phi_l}{I(q)} = \frac{(1+h)}{v_l\langle N_l\rangle_w h}\left[1 + \frac{q^2(2+h)\langle R_g\rangle_n^2}{3h}\right] + 2A_2\phi_l \quad (12)$$

According to this equation, in the $\phi_l \rightarrow 0$ limit, a plot of $I(q)^{-1}$ versus q^2 should be linear and the radius of gyration, R_g, can be obtained from the slope. On the basis of eq 12, $\phi_l/I(q)$ versus q^2 can also be cross-plotted for different concentration samples, which is the classical Zimm plot.[24,25] The extrapolated $\phi_l/I(0)$ data plotted versus ϕ_l should be linear, and the second virial

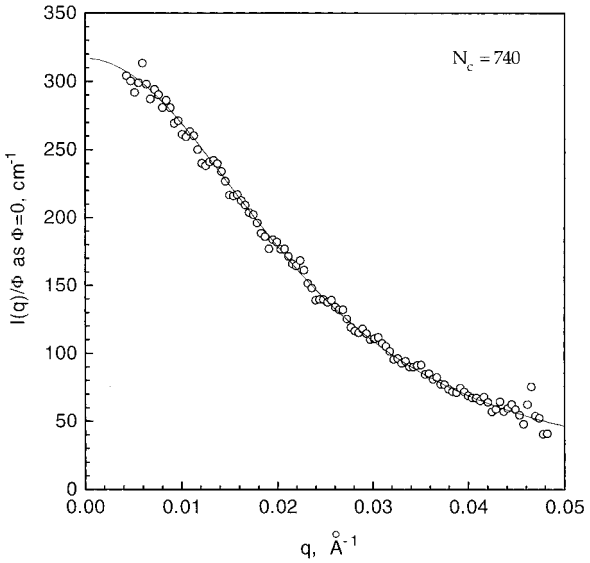

Figure 4. Zero concentration extrapolated scattering versus q for the sample with $N_c = 740$.

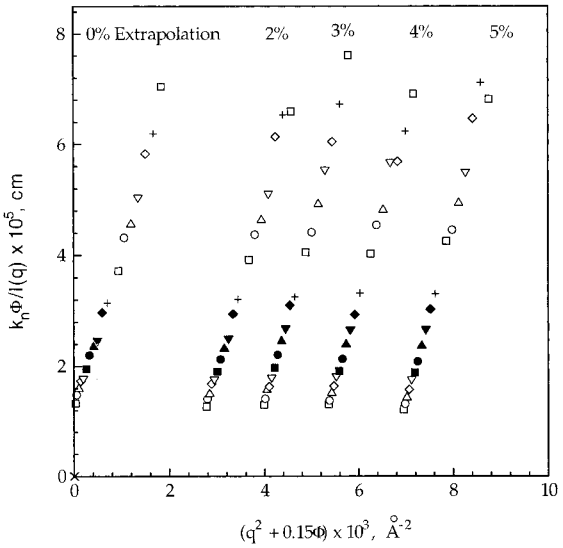

Figure 5. Zimm plot for samples with $N_c = 740$. The dashed line is the theoretical prediction.

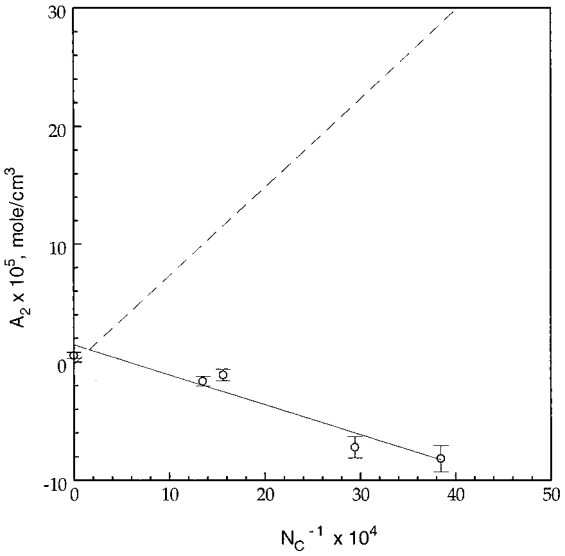

Figure 6. Second virial coefficient versus N_c^{-1}.

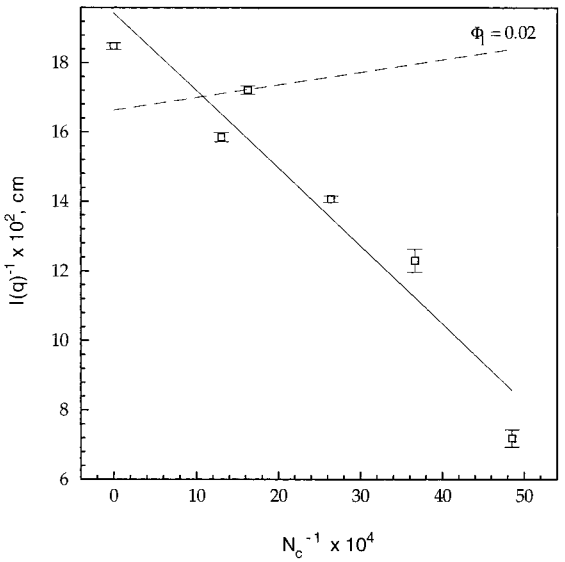

Figure 7. $I(0)^{-1}$ versus N_c^{-1} for the samples with linear chain concentration equal to 0.02. The dashed line is the theoretical prediction.

coefficient can be obtained. As an example, a classical Zimm plot for the samples with $N_c = 740$ is given in Figure 5. For the single phase samples, values for A_2 were obtained as a function of crosslink density and the results are listed in Table 1. A plot of the measured A_2 versus N_c^{-1} is given in Figure 6, and the solid line is the linear least squares fit to the data. The experimental observation is that A_2 decreases with increasing crosslink density (or decreasing N_c). As discussed earlier, the phase separation indicated by the decreasing A_2 cannot be explained by classical theory, as eq 4 predicts the opposite dependence of A_2 with N_c. The theoretical prediction from eq 4 is shown as a dashed line in Figure 6.

According to eq 2, a plot of $I(0)^{-1}$ versus N_c^{-1} for same linear chain concentration samples also gives a straight line. A typical plot of $I(0)^{-1}$ versus N_c^{-1} for $\phi_1 = 0.0177$ is given in Figure 7. The solid straight line was the linear least squares fit to the experimental data. The predicted scattering based on eq 2 was plotted in Figure 7 as the dashed line. The calculated line in Figure 7 also has a slope which is opposite to the data, similar to the results predicted in Figure 6 for A_2. The analysis of both A_2 and $I(0)$ based on classical theory ignores any possible dependence of χ on the crosslink density which has been observed in some systems,[48,49] although this effect is expected to be small in comparison with the observed trends.

The difference between the calculated and measured values of A_2 and $I(0)^{-1}$ has been observed previously. Briber and Bauer[41] discussed this difference as a failure of classical Gaussian rubber elasticity to adequately describe the zero angle scattering. Gaussian rubber elasticity predicts that as the crosslink density increases (N_c decreases), the scattering should decrease. At a fixed temperature, as the crosslink density increases, theory predicts that the value of $(\chi - \chi_s)$ should increase causing a decrease in $I(0)$. This is not what is observed experimentally. It remains to be seen if other theories for rubber elasticity can explain the experimental results.

An alternate explanation has been proposed by Bastide et al.,[50] where the excess scattering intensity (from the swollen network) is due to a nonuniform density of crosslinks. Regions of nonuniform crosslink density exist due to sample preparation, and subsequent swell-

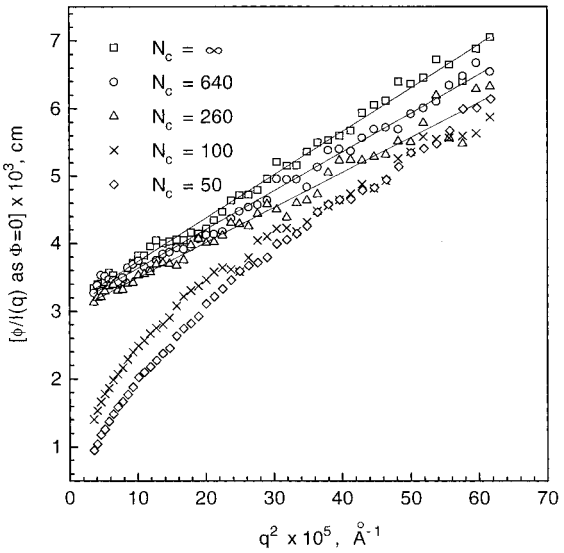

Figure 8. $I(q)^{-1/2}$ versus q^2 for the zero concentration extrapolated data for five different crosslink density samples.

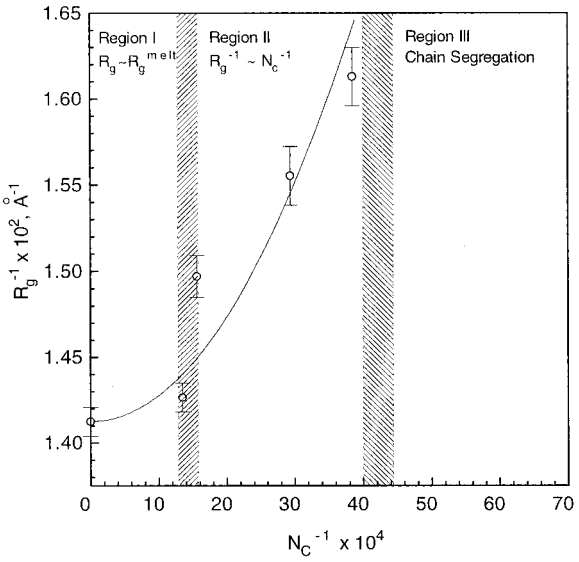

Figure 9. R_g^{-1} versus N_c^{-1}.

ing allows the observation of these regions by scattering. Although crosslink density may be nonuniform in these networks, it seems unlikely that it would affect the scattering as strongly as is observed at the very low effective degree of swelling studied in this work. Recently, Rabin and Onuki[51] have proposed that the fundamental assumptions of classical rubber elasticity where the free energy of the gel is the sum of an elastic strain energy and mixing free energy (with the free energy of mixing for the swelling species being the same as that for an identical polymer blend) is not valid. The difference between the theoretical prediction and the experimental data observed in this work and others[41,49] could indicate that the basic assumptions of the classical theory may be questionable. Also recent work by Fredrickson et al.[52,53] shows that the presence of a crosslink dependent effective interaction parameter, χ, can be explained by molecular architecture differences in polymer blends of the same chemical species.

C. Radius of Gyration as a Function of Crosslink Density. For the samples which remained in the single phase state, the zero concentration extrapolated data can be plotted as $I(q)^{-1}$ versus q^2 to provide an easy method for observing R_g (eq 12). Figure 8 is a plot of the extrapolated zero concentration scattering data for five different crosslink density samples. The solid lines are linear least squares fits to the data sets which show linear behavior. The slope of the straight lines decrease as the crosslink density increases, indicating that R_g for the linear chains decreases as N_c decreases. For samples with higher crosslink densities, the scattering increases dramatically in the low-q region (and no longer shows linear $I(q)^{-1}$ versus q^2 behavior), indicating that the linear chains have segregated.

Figure 9 shows the radius of gyration as a function of the crosslink density. The solid line in Figure 9 is the theoretical prediction by eq 8, and the constant, C, in eq 8 was found to be 77.2 molecule^{-2}, which can be related to the dimensionless pseudopotential of the random obstacles. Three different regimes can be distinguished in Figure 9. The first region corresponds to where the mesh size of the network is larger than the length of the linear chain ($N_c > N_l$), and no change in the linear chain radius of gyration as a function of crosslink density is observed. The theoretical prediction in this region also shows a very slow change of radius of gyration as a function of crosslink density. The second region occurs when the network mesh size is less than the length of the linear chain ($N_c < N_l$) and a systematic decrease in the radius of gyration is observed as a function of the crosslink density. In this region, the scaling law predicted by eq 9 is observed as expected if the crosslink points are acting like random obstacles influencing the radius of gyration of the linear chain. The third region occurs when the mesh size is much smaller than the length of the linear chain ($N_c << N_l$) and segregation of linear chains is observed. This segregation is clearly shown by the non-Gaussian scattering (nonlinear) behavior observed in Figure 8. This region corresponds to the samples where the chains have segregated. Computer simulations have found[19] the shape of the polymer linear chain in a porous medium is considerably more spherical (less anisotropic) than typical random Gaussian coils. The experiments discussed in this paper do not provide information on the anisotropy in the shape of the segregated polymer chains. This third region should probably correspond to a metastable state. If the system were in equilibrium, the network would shrink and linear chains would be expelled from the network.[54] This kind of phase separation between the network and the swelling agent (sometimes called microsyneresis) has been observed before in network/solvent systems.[54] For the system discussed in this paper, the process of expelling the linear chain from the network should be very slow and chains probably become trapped in regions of the network with lower crosslink density.

The contraction (or expansion) of the polymer chain relative to its Gaussian state can be described by an expansion factor, α, defined as[28] $\alpha \equiv R_g/R_g(\Theta)$, where R_g is the observed radius of gyration and $R_g(\Theta)$ is the radius of gyration in the theta state. In this study, R_g is taken as the radius of gyration of linear chain in a crosslinked matrix and $R_g(\Theta)$ is taken as the radius of gyration of the linear chain in the uncrosslinked matrix. The calculated values of α as a function of crosslink density are listed in Table 1. The values of α observed here prior to segregation of the chains are in the same range as those found for the collapse transition for linear polystyrene in dilute solution.[56]

D. Analysis of Two Phase Samples. For the higher crosslink density samples, the nonlinear behavior

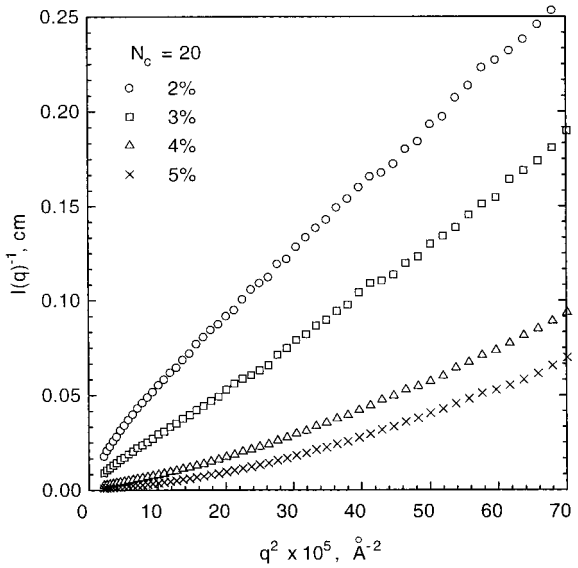

Figure 10. Ornstein−Zernike plot for samples with $N_c = 20$.

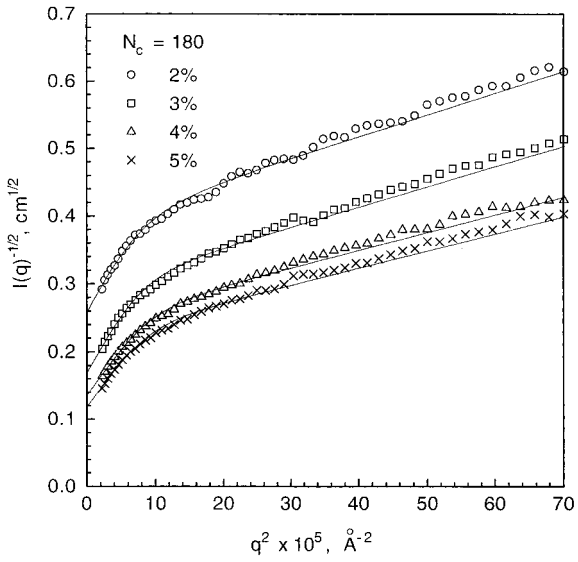

Figure 11. $I(q)^{-1/2}$ versus q^2 plot and nonlinear best fit curves for the samples with $N_c = 180$.

at the low-q region of the Ornstein−Zernike plots implies that the free chains have segregated and are not dispersed uniformly. This is also the behavior exhibited by most of the samples studied by Wu and Jong, where a decrease in the R_g of the linear chain was observed in the segregated regions using SANS and contrast variation.[22] The curvature of $I(q)^{-1}$ versus q^2 plots in the low-q region changes with linear chain concentration and crosslink density for all of the phase separated samples. In general, the curvature changes from concave downward to convex upward with increasing crosslink density at fixed linear chain concentration (Figure 10).

Based on the Debye−Bueche equation for a two phase structure with sharp interfaces, a plot of $I(q)^{-1/2}$ versus q^2 should be a straight line. As an example, a plot of $I(q)^{-1/2}$ versus q^2 for the samples with $N_c = 180$ is given in Figure 11. The data in this plot show relatively linear behavior in the high-q region and a significant deviation from linearity in the low-q region. In general, for a given crosslink density, the low-q curvature decreases with increasing linear chain concentration. This nonlinear behavior in the $I(q)^{-1/2}$ versus q^2 plot demonstrates that the structure of these samples does not fit the Debye−Beuche model. The changing curvature in the $I(q)^{-1/2}$ versus q^2 plot in the low-q region has been observed before for other systems[37−39] and can be analyzed using a two-correlation length scattering model.[37] This model is summarized in the theoretical section, and the scattering intensity is given by eq 11. The first term in eq 11 is the normal Debye−Bueche term, and the second term is Guinier type scattering.[57] According to this equation the sum of B_1 and B_2 equals $I(0)$. Nonlinear regression fitting of the data can be performed using eq 11 by floating three parameters, B_1, ξ_1, and ξ_2 with the constraint that $B_2 = [I(0) - B_1]$. The zero angle scattering intensities were obtained by Guinier extrapolation of the low-q scattering data to $q = 0$ ($\ln[I(q)]$ versus q^2).[57] The best fit curves are presented in Figure 11 as solid lines. The model was found to fit the data quite well. The best fit parameters B_1, ξ_1, and ξ_2 are listed in Table 2. If we assume that in the phase separated samples the segregated linear polymer forms spherical particles, the average size $\langle l_c \rangle$ and the average volume $\langle v \rangle$ of the particles can be calculated, and the values are also given in Table 2.

In the two-correlation length model, the correlation length, ξ_1, is the short-range correlation length and, ξ_2, is the long-range correlation length. ξ_1 is related to the average size of the primary particle, and ξ_2 is related to the average cluster size of the primary particles. Plots of ξ_1 and ξ_2 as a function of linear chain concentration and crosslink densities are given in Figures 12 and 13, respectively. Figure 12 shows that at constant crosslink density, ξ_1 increases with increasing linear chain concentration while ξ_2 is relatively constant. Figure 13 shows that at constant linear chain concentration both ξ_1 and ξ_2 decrease with decreasing crosslink density.

The parameter f is defined as the fractional contribution of the exponential correlation function to the total scattering. It was found that f decreases with increasing linear chain concentration for samples with the same crosslink density and when the crosslink density increases for the samples with the same linear chain concentration. The behavior of ξ_1, ξ_2, and f as a function of linear chain concentration is consistent with a model of segregated chains in regions which increase in size and contain more chains as the concentration increases.

The extrapolated zero angle intensity ($I(0) = B_1 + B_2$) from Table 2 indicates that the segregated chains consist of aggregates of multiple chains. The number of chains can be estimated by dividing $I(0)$ for the segregated samples by the expected $I(0)$ if chains were uniformly dispersed. For example, the number of aggregated chains varies from about 2 to 5 as the concentration varies from 2 to 5% for the samples with $N_c = 180$. Clearly, as the crosslink density increases, it becomes unfavorable for the linear chains to remain dispersed, though the network and aggregation occur. This aggregation process occurs during the polymerization of the network around the linear chains and probably results in a morphology which is non-equilibrium with the linear chains trapped in regions of lower crosslink density. Annealing of the samples was performed after the synthesis to allow the linear chains to reach equilibrium, but this may not be possible due to the low mobility of the chains in a crosslinked matrix.

Conclusions

The chain conformation of linear polystyrene trapped in a polystyrene network has been studied by small

Table 2. Results from the Two-Correlation Length Model

sample N_c	B_1, cm^{-1}	B_2, cm^{-1}	ξ_1, Å	ξ_2, Å	f	$\langle l_c \rangle$, Å	$\langle \nu \rangle \times 10^{-3}$, Å^3
180 (2%)	6.7 ± 0.2	8.4 ± 0.7	29.0 ± 0.8	317 ± 12	0.996 ± 0.0001	60.3 ± 1.6	440 ± 31.0
180 (3%)	11.7 ± 0.3	23.8 ± 1.4	32.0 ± 0.8	348 ± 10	0.993 ± 0.0002	67.9 ± 1.6	800 ± 50.9
180 (4%)	16.8 ± 0.5	38.3 ± 2.7	32.8 ± 0.9	338 ± 8	0.991 ± 0.0003	70.5 ± 1.8	920 ± 52.6
180 (5%)	20.4 ± 0.6	51.5 ± 4.1	33.9 ± 0.9	349 ± 8	0.990 ± 0.0003	73.3 ± 1.8	1080 ± 61.4
100 (2%)	9.7 ± 0.4	29.8 ± 2.5	34.0 ± 1.2	361 ± 9	0.989 ± 0.0005	74.6 ± 2.4	1260 ± 84.7
100 (3%)	13.1 ± 0.5	37.7 ± 3.0	32.2 ± 1.3	361 ± 11	0.991 ± 0.0004	69.6 ± 2.6	1030 ± 80.8
100 (4%)	23.6 ± 1.0	88.6 ± 7.7	39.1 ± 1.6	372 ± 8	0.981 ± 0.0008	89.4 ± 3.2	2230 ± 146
100 (5%)	36.2 ± 1.4	127 ± 13.5	41.5 ± 1.5	366 ± 7	0.978 ± 0.0008	95.9 ± 3	2520 ± 144
50 (2%)	11.6 ± 0.5	43.3 ± 4.5	38.5 ± 1.5	373 ± 9	0.982 ± 0.0008	87.6 ± 3	2120 ± 148
50 (3%)	22.9 ± 0.8	82.6 ± 9.3	43.1 ± 1.3	376 ± 7	0.976 ± 0.0008	100 ± 2.6	2870 ± 158
50 (4%)	33.3 ± 1.3	116 ± 15.8	44.8 ± 1.5	378 ± 7	0.974 ± 0.0010	104 ± 3	3150 ± 181
50 (5%)	55.3 ± 1.8	177 ± 18.7	50.1 ± 1.4	382 ± 6	0.968 ± 0.0010	118 ± 2.8	4090 ± 196
20 (2%)	22.7 ± 0.8	71.0 ± 8.0	46.0 ± 1.4	378 ± 7	0.975 ± 0.0009	105 ± 2.8	3100 ± 170
20 (3%)	54.0 ± 1.3	128 ± 15.7	57.2 ± 1.0	385 ± 5	0.966 ± 0.0008	133 ± 2.0	4880 ± 173
20 (4%)	387 ± 4.6	483 ± 54.4	87.1 ± 0.6	472 ± 6	0.968 ± 0.0004	196 ± 1.2	11200 ± 260
20 (5%)	935 ± 2.0	1160 ± 118	96.7 ± 1.2	423 ± 6	0.937 ± 0.0001	228 ± 2.3	15200 ± 440

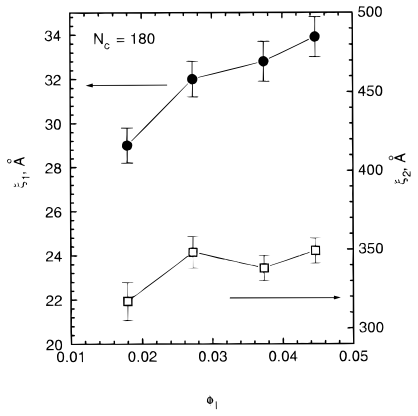

Figure 12. Correlation lengths ξ_1 and ξ_2 as a function of concentration for samples with $N_c = 180$.

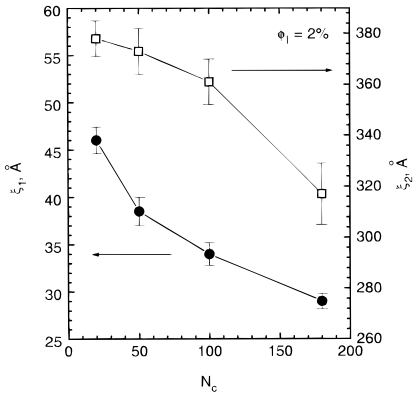

Figure 13. Correlation lengths ξ_1 and ξ_2 as a function of crosslink density for samples with $\phi_l = 0.02$.

angle neutron scattering for a wide range of crosslink densities. It was found that the lower crosslink density samples were single phase, but the higher crosslink density samples were phase separated. The phase separation occurred during the polymerization of the network and probably trapped the segregated chains in a non-equilibrium state. For the single phase samples the radius of gyration of the linear chains, R_g, was found to be a function of the crosslink density. When the crosslink density was low ($N_c > N_l$), R_g did not change appreciably, but as the crosslink density increased ($N_c < N_l$), R_g decreased according to the scaling relation $R_g^{-1} \sim N_c^{-1}$ as predicted by arguments based on the collapse of a polymer chain in a field of quenched random obstacles where the obstacles are equated to the crosslink points of the network. The decrease in R_g observed as the crosslink density increased is about 15%, comparable to what has been observed for the collapse transition for chains in dilute solution. The second virial coefficient was found to decrease with increasing crosslink density, which does not agree with classical theory. For the phase separated samples it was found that, with increasing linear chain concentration or crosslink density, the degree of segregation of the linear chains increased. The segregated linear chains were not uniformly distributed in the samples, and the degree of nonuniformity was controlled by the crosslink density.

References and Notes

(1) de Gennes, P. G. *J. Chem. Phys.* **1971**, *53*, 572.
(2) Cassasa, E. F. *Macromolecules* **1976**, *9*, 182.
(3) Ageev, E. P.; Vershubskii, A. V. *Russ. J. Phys. Chem.* **1995**, *69*, 1004.
(4) Aminabhavi, T. M.; Khinnavar, R. S. *Polymer* **1993**, *34*, 1006.
(5) Antonietti, M.; Sillescu, H. *Macromolecules* **1985**, *18*, 1162.
(6) Antonietti, M.; Coutandin, J.; Sillescu, H. *Macromolecules* **1986**, *19*, 793.
(7) Anderson, J. L.; Quinn, J. A. *Biophys. J.* **1974**, *14*, 130.
(8) Zheng, X.; et al. *Macromolecules* **1993**, *26*, 6431.
(9) Deutsch, J. M. *Science* **1988**, *240*, 922.
(10) Brochard, F.; de Gennes, P. G. J. *Chem. Phys.* **1977**, *67*, 52.
(11) Viovy, J. L.; Jesec, J. *Advances in Polymer Science*; Springer-Verlag: Berlin, Heidelberg, 1994; Vol. 114, p 1.
(12) Thirumalai, D. *Phys. Rev. A* **1988**, *37*, 269.
(13) Duplantier, B. *Phys. Rev. A* **1988**, *38*, 3647.
(14) Muthukumar, M. *J. Chem. Phys.* **1989**, *90*, 4594.
(15) Douglas, J. F. *Macromolecules* **1988**, *21*, 3515.
(16) Edwards, S. F.; Muthukumar, M. *J. Chem. Phys.* **1988**, *89*, 2435.
(17) Baumgärtner, A.; Muthukumar, M. *J. Chem. Phys.* **1987**, *87*, 3082.
(18) Gersappe, D.; Deutsch, J. M.; Olvera de la Cruz, M. *Phys. Rev. Lett.* **1991**, *66*, 731.
(19) Honeycutt, J. D.; Thirumalai, D. *J. Chem. Phys.* **1989**, *90*, 4542.
(20) Lee, B. S.; Nakanishi, H. *Phys. Rev. Lett.* **1988**, *61*, 2022.
(21) Boué, F.; Farnoux, B.; Bastide, J. *Europhys. Lett.* **1986**, *1* (1), 637.
(22) Wu, W. L.; Jong, L. *Polymer* **1993**, *34*, 2357.
(23) Horkay, F.; et al. *Macromolecules* **1995**, *28*, 678.
(24) Zimm, B. H. *J. Chem. Phys.* **1948**, *16*, 1093.
(25) Zimm, B. H. *J. Chem. Phys.* **1948**, *16*, 1099.
(26) Hadziioannou, G.; Stein, R. S. *Macromolecules* **1984**, *17*, 567.
(27) Jahshan, S. N.; Summerfield, G. C. *J. Polym. Sci.: Polym. Phys. Ed.* **1980**, *18*, 1858.
(28) Flory, P. J. *Principles of Polymer Chemistry*; Cornell University Press: Ithaca, NY, 1953.
(29) Flory, P. J.; Rehner, J. *J. Chem. Phys.* **1943**, *11*, 521.
(30) Bauer, B. J.; Briber, R. M.; Han, C. C. *Macromolecules* **1989**, *22*, 940.
(31) Sakurai, S.; Hasegawa, H.; Hashimoto, T.; Han, C. C. *Polym. Commun.* **1990**, *31*, 99.
(32) Maconnachie, A.; Kambour, R. P.; White, D. M.; Rostami, S.; Walsh, D. J. *Macromolecules* **1984**, *17*, 2645.
(33) Schulz, G. V. Z. *Phys. Chem., Abt. B* **1939**, *B43*, 25.
(34) Mori, K.; Tanaka, H.; Hasegawa, H.; Hashimoto, T. *Polymer* **1989**, *30*, 1389.

(35) Debye, P.; Anderson, H. R.; Brumberger, H. *J. Appl. Phys.* **1957**, *28*, 679.
(36) Fernandez, A. M.; Wignall, G. D.; Sperling, L. H. *Adv. Chem.* **1986**, *211*, 10.
(37) Moritani, M.; Inoue, T.; Motegi, M.; Kawai, H. *Macromolecules* **1970**, *3*, 433.
(38) Cheung, Y. W.; Stein, R. S.; Wignell, G. D.; Yang, H. E. *Macromolecules* **1993**, *26*, 5365.
(39) Wignall, G. D.; Farrar, N. R.; Morris, S. *J. Mater. Sci.* **1990**, *25*, 69.
(40) Certain commercial materials and equipment are identified in this paper in order to specify adequately the experimental procedure. In no case does such identification imply recommendation or endorsement by the National Institute of Standards and Technology (NIST) nor does it imply that they are necessarily the best available for the purpose.
(41) Briber, R. M.; Bauer, B. J. *Macromolecules* **1991**, *24*, 1899.
(42) Barton, A. F. M. *Handbook of Polymer-Liquid Interaction Parameters and Solubility parameters*; CRC Press: Cleveland, OH, 1990.
(43) Higgins, J. S.; Benoît, H. *Polymers and Neutron Scattering*; Clarendon Press: Oxford, U.K., 1994.
(44) Barford, N. C. *Experimental Measurements: Precision, Error and Truth*; Wiley and Sons: New York, 1985.
(45) de Gennes, P. G. *J. Phys. (Paris)* **1970**, *31*, 235.
(46) de Gennes, P. G. *Scaling Concepts in Polymer Physics*; Cornell University Press: Ithaca, NY, 1979.
(47) Londono, J. D.; Narten, A. H.; Wignall, G. D.; Honnel, K. G.; Hsieh, E. T.; Johnson, T. W.; Bates, F. S. *Macromolecules* **1994**, *27*, 2864.
(48) Stanley, H. E. *Introduction to Phase Transitions and Critical Phenomenon*; Oxford University Press: New York, 1971.
(49) McKenna, G. B.; Flynn, K. M.; Chen, Y. H. *Polym. Commun.* **1988**, *29*, 272.
(50) Bastide, J.; Leibler, L.; Prost, J. *Macromolecules* **1990**, *23*, 1821.
(51) Rabin, Y.; Onuki, A. *Macromolecules* **1994**, *27*, 870.
(52) Fredrickson, G. H.; Liu, A.; Bates, F. S. *Macromolecules* **1994**, *27*, 2503.
(53) Fredrickson, G. H.; Briber, R. M.; Leibler, L. Manuscript in preparation.
(54) Brochard, F. *J. Phys. (Paris)* **1981**, *42*, 505.
(55) Zrinyi, M.; Wolfram, E. *J. Colloid Interface Sci.* **1980**, *90*, 34.
(56) Park, I. H.; Wang, Q. W.; Chu, B. *Macromolecules* **1987**, *20*, 1965.
(57) Guinier, A.; Fournet, G. *Small-Angle Scattering of X-rays*; Wiley: New York, 1955.
(58) *National Instutiute of Standards and Technology Cold Neutron Research Facility 30m SANS Instruments Data Acquisition Manual*; National Institute of Standards and Technology: Washington, D.C., June 1996.

MA960864Y